PRINCIPLES OF HEAT TRANSFER MODELLING USING THERMOCHROMIC LIQUID CRYSTALS AND LASER ANEMOMETRY

M.JEWARTOWSKI, J.STASIEK[c]

Department of Energy and Industrial Apparatus, Gdansk University of Technology, Gdansk, 80-233, Poland

[c]Corresponding author: Tel.: +48 58 347 2516; Fax: +48 58 347 2816; Email: jstasiek@pg.gda.pl

KEYWORDS:

Main subjects: heat and mass transfer, flow visualization
Fluid: turbulence flow, vortex generators
Visualization method(s): liquid crystal thermography, particle image velocimetry
Other keywords: true colour image processing

ABSTRACT: In the last two decades thermochromic liquid crystals (TLC) and true-colour digital image processing have been successfully used in non-intrusive technical, industrial and biomedical studies and applications. Thin coatings of TLC's at surfaces are utilized to obtain detailed temperature distributions and heat transfer rates for steady or transient processes. Liquid crystals also can be used to make visible the temperature and velocity fields in liquids by the simple expedient of directly mixing the liquid crystal material into the liquid (water, glycerol, glycol, and silicone oils) in very small quantities to use as thermal and hydrodynamic trawers. Two experimental techniques were employed in the research. Firstly, the steady-state liquid crystal technique was used to determine the distribution of surface temperature and subsequent evaluation of heat transfer coefficient. Secondly, the PIV (Particle Image Velocimetry) method was employed to study the flow pattern produced by transverse vortex generators, visualized using a planar beam of double-impulse laser tailored by a cylindrical lens and oil particles. Apart from the heat transfer data the pressure drop was also measured.

INTRODUCTION: The discovery of cyanobiphenyl liquid crystals by Gray et al. [1], the evaluation of their properties at the Royal Signals & Radar Establishment and their commercialization by BDH (now Merck Ltd) revolutionized liquid crystal (LC) technology and made possible dramatic advances in liquid crystal displays technology over the last two decades. Also, the development of LC technique for temperature and temperature gradients measurement over the past 20 years, coupled with digital image processing, has opened some new approaches for technical and biomedical thermographic research. During the same period, there has been an increasing use of desktop computers in scientific and industrial applications, first to facilitate conventional experiments and then to expand the range of possible experiments. These two new tools have come together during the past 20 years to produce a powerful new experimental technique: true-colour digital processing of liquid crystal images to yield full-field measurements of temperature, heat transfer coefficient distributions, as a judgment of food quality, and for electronic components and colour photographs, among other applications.

Swirl, flow destabilization and developing viscous layers are commonly regarded as three passive ways to influence heat transfer due to the presence of vortices and their generation. Their capability is to intensify heat transfer even by several hundred percent in selected cases. In order to appropriately devise the flow turbulizers fundamental knowledge is required on the issue of how different devices contribute to vortex generation, their control and how they interact with the original or base flow and temperature field. Selection of the most appropriate vortex generators (VG)

for a given task requires prior knowledge of the heat transfer and flow losses associated with the generation of a specific vortex system.

Vortices swirl fluid around their axis of rotation, they induce velocity profiles which are less stable, and their generation implies flow separation and developing viscous layers [2,3,4]. Vortices do not only contribute to swirl but also destabilize the flow. That is well known as the transverse vortices (TV). The Karman vortex street behind a cylinder in the cross flow is probably the best known example. The destabilization effects of longitudinal vortices (LV) are still under investigation. One of the reasons is that single LVs are more difficult to generate than TVs. Self-sustained oscillations associated with vortices have been exploited very little in general and specially for heat transfer purposes. The third mechanism, i.e. viscous layer interruption and initiation of new developing viscous layers is implied by vortex generation (VG).

Many parameters affect the performance of rib channels equipped with turbulising ribs. These are the shape and dimensions of the channel (including constant and variable cross section channels and multiple sharp turns), the rib characteristics (including shape, size, location and thermal conductivity) and convective flow characteristics (Reynolds and Prandtl numbers). Among these parameters, the most important role is played by the rib placement and for that reason there is a considerable amount of literature on that topic for evaluation of heat transfer and friction characteristics of stationary straight channels with various forms of turbulizers.

An important issue in the experimental heat transfer investigation of ribbed channels is the adopted measuring technique. A large number of investigations have been performed by the standard technique which uses heater plates/foils and thermocouples [5,6,7,8] or the naphthalene sublimation technique [9,10] as well as infrared thermographic technique [11,12] and the liquid crystal thermography (LCT) technique [13,14].

In this paper measurements of local heat transfer coefficients in a rib-roughened rectangular channel are presented. Many parameters affect the performance of rib-roughened channels: the shape and dimentions of the channel (including constant and variable cross section channels and multiple sharp turns), the rib characteristics (including shape, size, location and thermal conductivity) and the rotation of the blade. Liquid crystals were used to determine the distribution of the surface temperature, and then evaluation of the heat transfer coefficient or the Nusselt number. The flow pattern produced by transverse vortex generators was visualized using a planar beam of double-impulse laser tailored by a cylindrical lens and oil particles. Sequential images of the particles in a cross sectional plane taken with CCD video camera from the downstream side the flow ware stored on a personal computer to obtain distributions of velocity vectors by means of the PIV method.

LIQUID CRYSTAL THERMOGRAPHY WITH SOME APPLICATIONS: Thermochromic liquid crystals (TLC) and true-color digital image processing have been successfully used in nonintrusive technical, industrial and biomedical studies and applications [15]. Thin coatings of TLC's at surfaces are utilized to obtain detailed temperature distributions and heat transfer rates for steady or transient processes. For flow analysis the suspension of thermochromic liquid crystals can be used to make visible the temperature and velocity fields in liquids. By dispersing the liquid crystal material into the liquid they become not only classical tracers used for flow visualization but simultaneously small thermometers monitoring local fluid temperature.

Liquid Crystals Thermography (so called LCT) have been extensively applied to the qualitative visualization of the entire steady state, or transient temperature fields on solid surfaces. Since quantifying color is a difficult and

somewhat ambiguous task, application of thermochromic liquid crystals initially was largely qualitative. Application of the color films or interference filters was tedious and inaccurate. The first application of true-color digital image processing gave impact to qualitative and fast temperature measurements. Rapid development of image processing techniques has made it now possible to set-up inexpensive systems capable of real-time transient full field temperature measurements using TLCs. Before the execution of a thermal or flow visualization experiment, we should recognize the characteristics of the overall combination of the TLC, the light source, the optical and camera system, and make a rational plan for the total measurement system. The relationship between the temperature of the crystal and the measured Hue of the reflected light defines the calibration curve for the specified liquid crystal [15]. The distribution of the color component pattern on the liquid crystal layer was measured by RGB color camera and a series of images at different temperatures defines the calibration. Fig . 1-5 demonstrate the application of liquid crystal thermography to some technical problems.

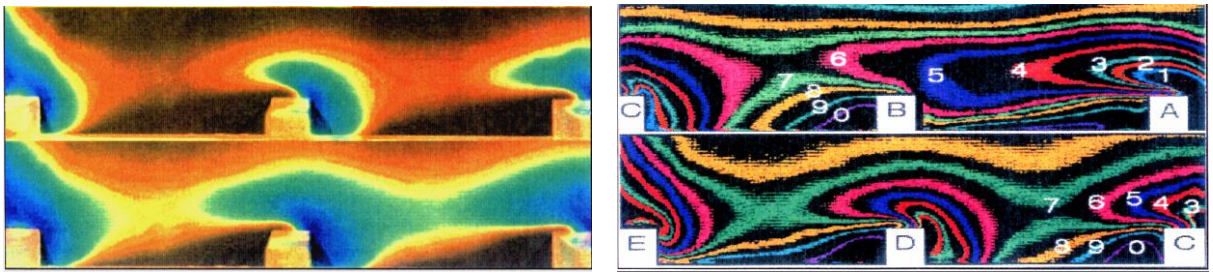

Fig. 1 True-colour images from liquid crystal thermography for an endwall surface with in-line square rigs (left) and pattern of 10 Nusselt numbers Nu reconstructed by false colour images of the heat transfer surface for Re=2000 (0: Nu=79; 9: 99, 8: 113, 7: 123, 6: 136, 5: 147, 4: 160, 3: 175, 2: 185, 1: 209) (right)

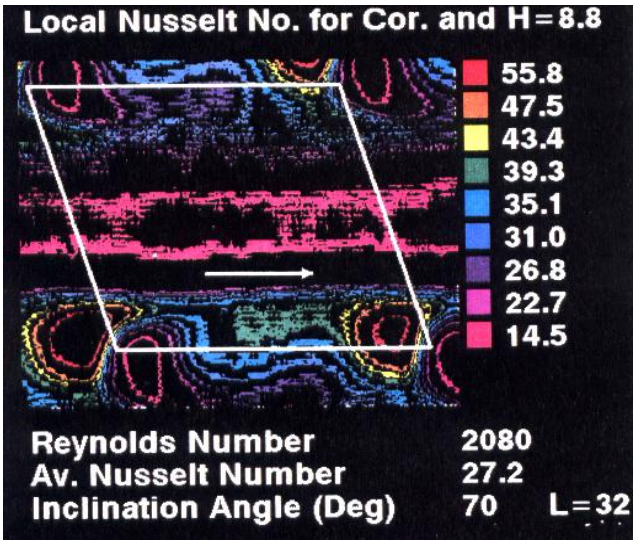

Fig. 2 False colour image of local Nusselt number contours over a central diamond of the undulated plate of corrugated-undulated geometry (ϕ = 70˚, Re = 2080, H=8.8 mm, L = 32 mm)

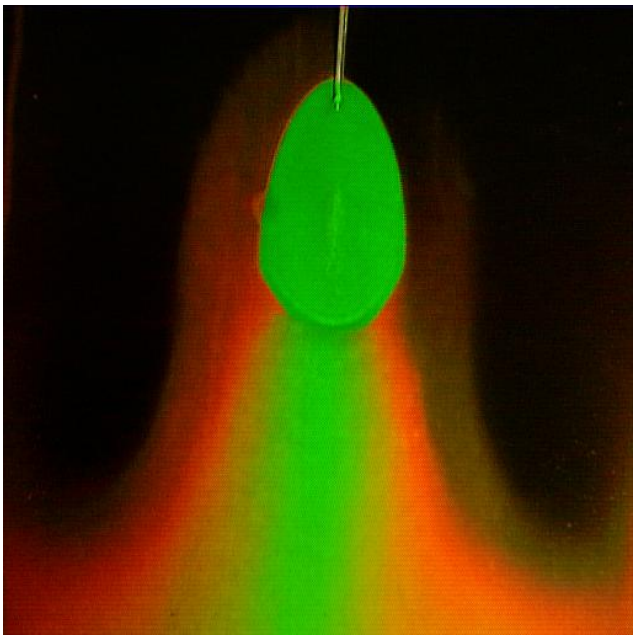

Fig. 3 True-colour image of water impinging jet on a liquid crystal-coated surface

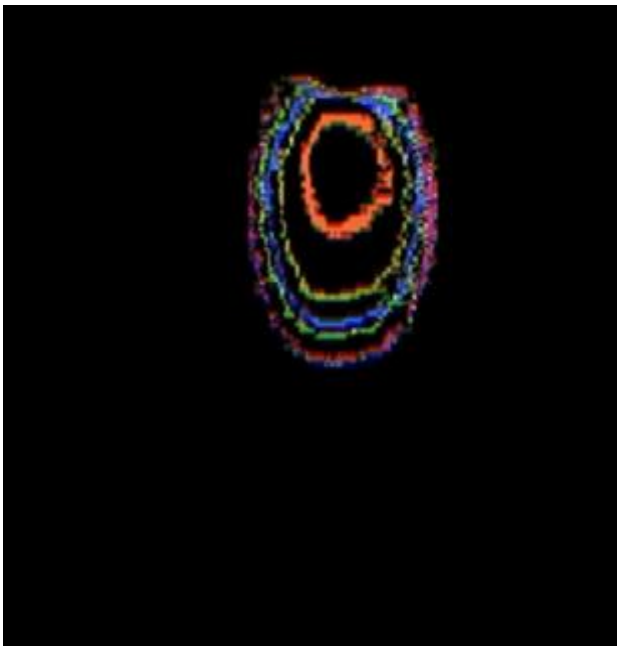

Fig. 4 False colour image of local Nusselt number contours for case from previous figure. Local Nusselt number: red-39.2, khaki-14.9, blue-11, green-9.1, violet-5.98. Nu_{av} – 15.03

Two main methods of surface temperature measurements are performed involving steady state and transient techniques. A brief history of these is given by Stasiek et al [15] and Baughn et al [16]. Steady-state with constant flux method has been used in the current experiment.

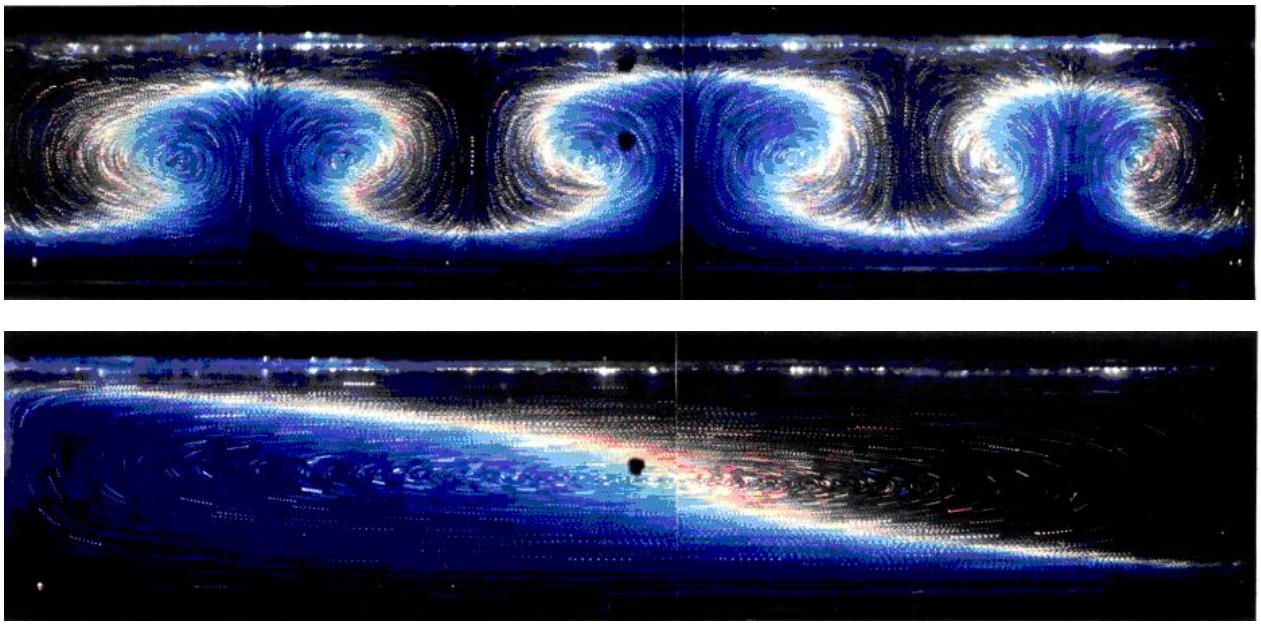

Fig. 5 Temperature and velocity visualization in glycerol-filled cavity under free convection using chiralnematic liquid crystal (Re = 12 000, Pr = 12 500)

EXPERIMENTAL APPARATUS AND PROCEDURE: The experimental study was carried out using an open low-speed wind tunnel consisting of entrance section with fan and heaters, large settling chambers with diffusing screen and honeycomb, and then working sections (Fig. 6). Air is drawn through the tunnel using a fan able to attain the Reynolds numbers in the range from 500 to 40 000. The working air temperature in the rig ranges from 15°C to 65°C produced by the heater or cooler positioned just downstream of the inlet. The major construction material of the wind tunnel is perspex. Local and mean velocity are measured using conventional Pitot tubes and DISA hot-wire velocity probe.

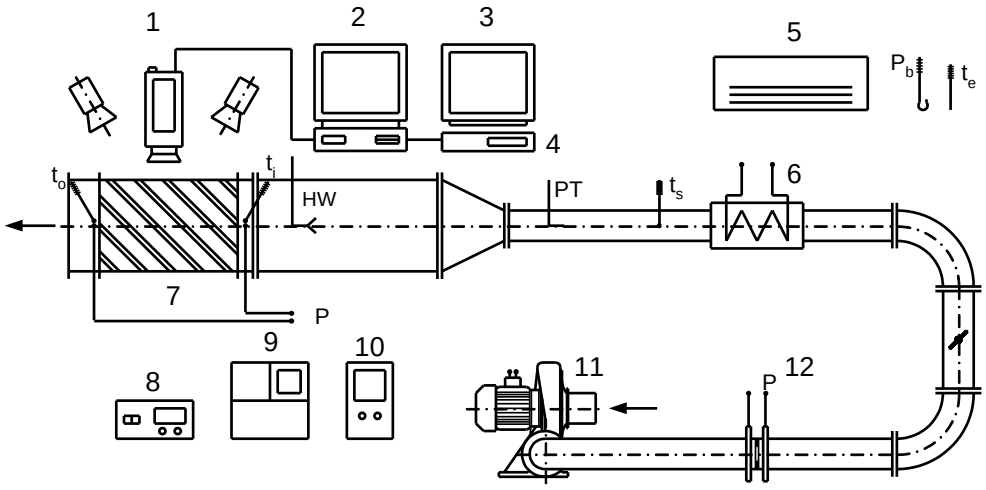

Fig. 6 Open low speed wind tunnel, 1 – RGB camera (TK-1070), 2 – PC, 3 – monitor (RGB-VMR 200), 4 – S-VHS recorder, 5 – air conditioning system, 6 – heater, 7 – LC mapping section, 8 – digital micro manometer FCO 12, 9 – DISA hot wire system, 10 – variac, 11 – fan, 12 – orifice

The alternative effects of constant wall temperature and constant heat flux boundary conditions are obtained using plate electric heater [17]. Photographs are taken using RGB video-camera and a true-color image processing technique. The liquid crystals used here, manufactured in sheet form by Merck Ltd [18], had an event temperature range from 30.0 to 35.0°C. In this particular experiment uncertainty for temperature measurement was estimated at about ± 0,05°C by considering only the section of the surface used in the experiment, span-wise non-uniformities in Hue value are minimized.

In many cases, as mentioned above, remarkable enhancement of local and spatially averaged surface heat transfer rates are possible with rib turbulators, in spite of the lower local Nusselt number at certain locations along the ribbed surfaces. Prior to ribbed turbulator test section is a 255x40 mm inlet duct that is 550 mm in length. This is equivalent to 7,96 hydraulic diameter (where the hydraulic diameter is 69,11 mm). The test surface that is analyzed contains a collection of rib turbulators that are perpendicular and angled with respect to the flow stream (Fig. 7). To determine the surface heat flux (used to calculate heat transfer coefficients and Nusselt numbers), the convective power levels provided by the thermofoil heaters are divided by flat test surface area. Spatially resolved temperature distributions along the bottom rib turbulator test surface are determined using liquid crystals thermography (LCT) and true-color image processing system commercially available from Data Translation Inc. [19].

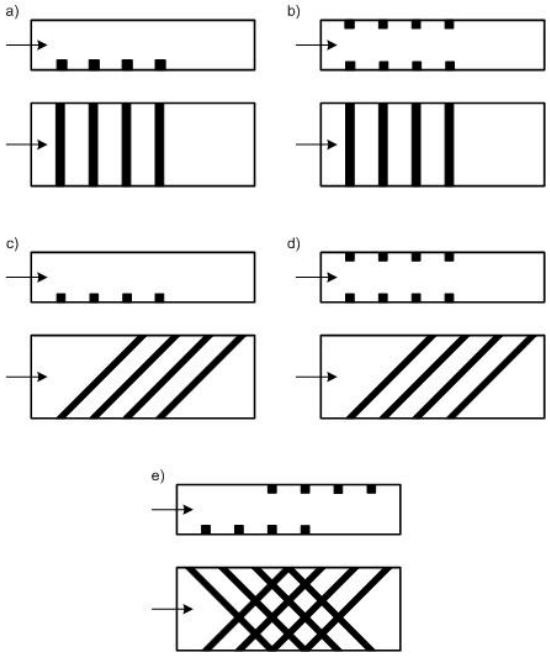

Fig. 7 Schematic view of five types of transverse vortex generators (cross-corrugated and rectangular ribs)

Particle Image Velocimetry

Particle Image Velocimetry technique is another well-established experimental method in fluid mechanics, that allows quantitative measurement of two-dimensional flow structure. It enables measurements of the instantaneous in-plane velocity vector field within a planar section of the flow field and allows to calculate spatial gradients, dissipation of turbulent energy, spatial correlations, and the like [20,21]. In PIV technique selected cross-section of the investigated seeded flow is illuminated by laser light formed in thin “light sheet” (Fig.8). Images of the flow are recorded by CCD camera and correlated to calculate instantaneous velocity fields.

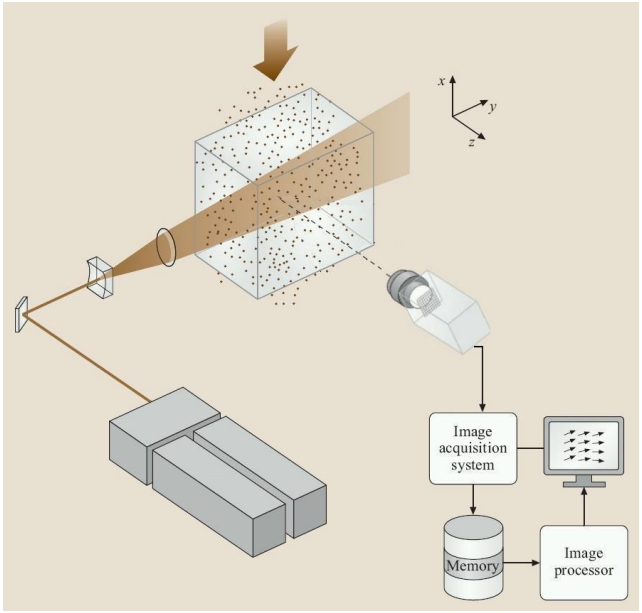

Fig. 8 Schematic of a typical PIV measurement system

The main part of the experimental set-up (Fig. 8) consists of a transparent model of ribbed channel, laser light source (30 mJ double pulse Nd:YAG laser SoloPIV, New Wave Research, Inc.) and high resolution 12bit digital CCD camera (1280 × 1024 pixels, PCO SensiCam). This system permits acquisition of two images at the minimum time interval of 200ns, exposition time of 5ns, and about 3.75Hz repetition rate. The PIV recording system installed on 3GHz Pentium 4 computer with 3GB RAM capable for acquisition over 200 pairs of images during a single experimental run.

The PIV measurements were performed for pure air seeded with small droplets (few micrometers in diameter) of synthetic oil DEHS (Di-Ethyl-Heksyl-Sebacat). The oil drops volumetric concentration was very low (< 0.001), hence they did not affect the flow structure.

RESULTS AND DISCUSSION: The heat transfer coefficient and the pressure drop per unit length are two of the most relevant parameters in the heat exchangers. This section presents measurement results of both parameters as well as velocity field obtained on model heat exchanger.

Results of LCT measurements

In the discussion that follows, the Nusselt number

$$Nu = h \cdot D_h / k \tag{1}$$

where h is the heat transfer coefficient, D_h is the channel hydraulic diameter and k is the molecular thermal conductivity of air.

The heat transfer coefficient is then based on the flat projected area and is determined using

$$h = q_n / (T_w - T_\alpha) \tag{2}$$

where q_n is the local (net) surface heat flux, local surface temperature T_w (found from LCT) and T_α is the time-averaged, local mixed mean air temperature.

The surface Nusselt number distribution along the rib turbulator test surface for four Reynolds number are presented in Fig 9 for one ribs geometry (b), which gave the best overall heat transfer enhancement. It is the evidence that transverse vortex generators (TVG_s) enhance heat transfer by several hundred percent but only for certain Reynolds

numbers. Comparison between the maps of velocity vectors and local Nusselt numbers contours reveals that high velocity do not enhance heat transfer in some cases, probably the moving fluid (with high velocity) does not penetrates into the boundary layer and flows above the ribs. Optimum flow condition should be established for high efficient enhancement of heat transfer augmentation in particular environment e.g. flow and heat exchanger configuration.

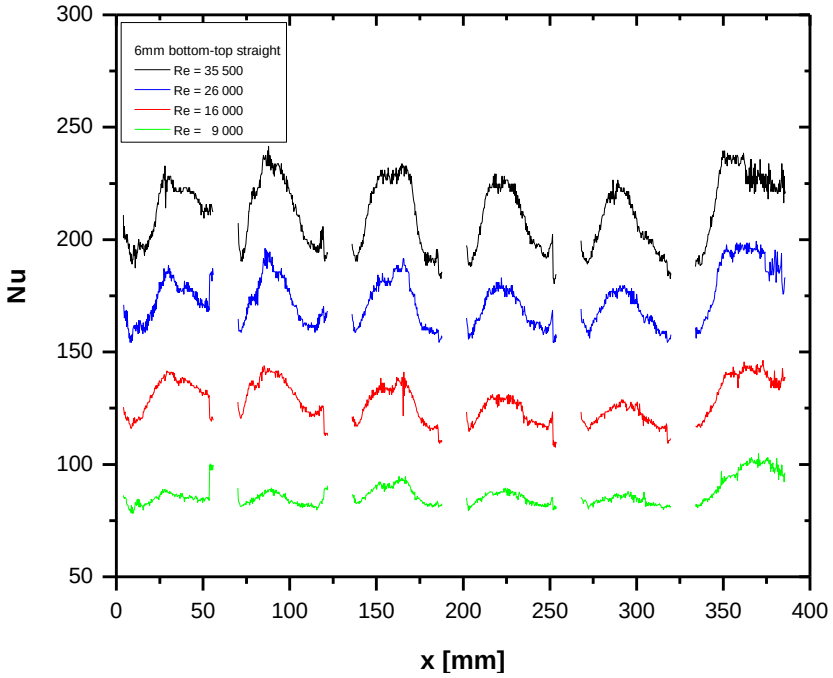

Fig. 9 Nusselt number distribution in consecutive test sections for different Reynolds numbers (Re=9000, 16000, 26000 and 35500) for geometry b

Table 1 Average Nusselt number and heat transfer coefficient distribution for different ribs geometry

Geometry	Re	h_{av}	Nu_{av}	Nu_o
a ribbed bottom wall, perpendicular	9000 16000 26000 35500	21.78 35.62 47.94 60.90	58.11 95.05 127.91 162.48	29 46 68 87
b ribbed bottom and top walls, perpendicular	9000 16000 26000 35500	31.71 45.97 63.00 77.88	84.60 122.65 168.10 207.78	29 46 68 87
c ribbed bottom wall, inclined at 45°	9000 16000 26000 35500	22.57 31.50 32.71 58.94	60.21 84.05 122.61 157.25	29 46 68 87
d ribbed bottom and top walls, inclined at 45°	9000 16000 26000 35500	22.42 32.47 48.70 60.54	59.82 86.64 129.93 161.53	29 46 68 87
e ribbed bottom and top walls, inclined at 45° “grating”	9000 16000 26000 35500	22.79 31.11 47.20 58.35	60.80 83.00 125.87 155.67	29 46 68 87

Table 1 presents average Nusselt number distribution as well as average heat transfer coefficient taken between 3rd and 4th rib for each geometry. For the purpose of comparison, calculations for the baseline condition of a smooth channel (without ribs) with asymmetric heating were performed. The local Nusselt number was normalized by the Nusselt number for fully developed turbulent flow in smooth circular tubes given by the well known Dittus-Boelter correlation:

$$Nu = 0.023 \cdot Re^{0.8} \cdot Pr^{0.4} \tag{3}$$

Nusselt number for smooth channel calculated according to Eq. (3) for given Reynolds numbers e.g. 9000, 16000, 26000 and 35500 results in the following data respectively: 29, 46, 68 and 87.

Results of PIV measurements

Velocity fields were obtained from the PIV measurements for different ribs geometries and different Reynolds numbers (Re = 9000, 16000 and 26000). The area interrogated by the PIV method was in all cases located in the mid-vertical-plane between side walls.

Fig. 10 shows average velocity field (averaged over 100 instantaneous velocity fields) and for geometry with ribbed bottom and top walls, perpendicular flow to ribs and Reynolds number Re = 16000. Maximum velocity for this case is about 5.5 m/s and is located in the middle part of the channel. Presented averaged velocity filed seems to be quite smooth but computed from 100 instantaneous velocity fields turbulence intensity (Fig.11), defined as:

$$TI = \frac{\left(\frac{1}{n}\sum_{i=1}^{n}(u_i - u_{av})^2\right)^{\frac{1}{2}}}{u_{av}} \cdot 100\% \tag{4}$$

Turbulence intensity field shows that this intensity achieves maximum value (about 60%) in the middle of the channel close to the ribs.

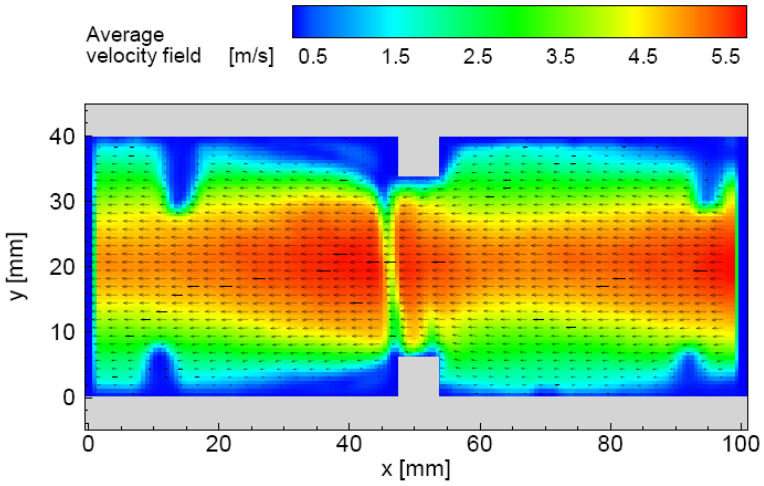

Fig. 10 Average velocity field for geometry with ribbed bottom and top walls, perpendicular flow to ribs and Reynolds number Re=16000

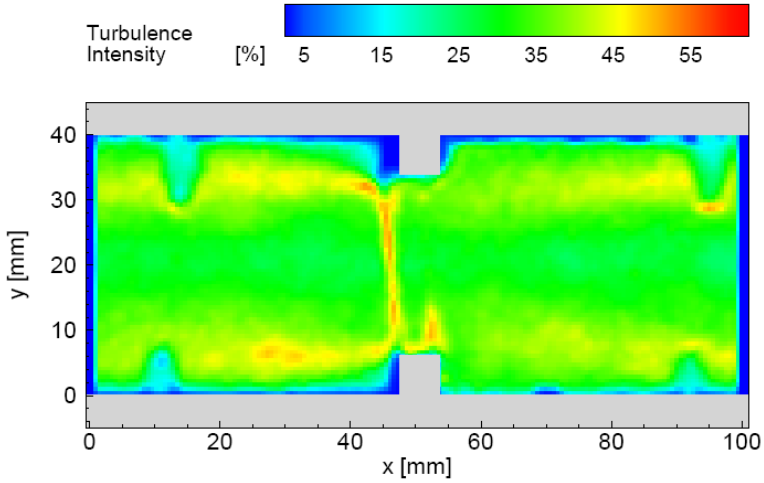

Fig. 11 Turbulence intensity for geometry with ribbed bottom and top walls, perpendicular flow to ribs and Reynolds number Re=16000

Results of pressure drop measurements

The behavior of equivalent friction coefficient f as a function of the Reynolds number for all five ribs configurations is presented in Fig. 12. Coefficient *f* was calculated for measured pressure drop from Darcy's formula [22]:

$$f = \frac{2 \cdot \Delta P \cdot D_h}{\rho \cdot u^2 \cdot l} \tag{5}$$

where ΔP is pressure lost, u – velocity and l – length.

High pressure drop corresponds to high Nusselt numbers. The biggest pressure drop as well as the highest average Nusselt number is for the geometry with ribbed bottom and top walls and perpendicular flow to the ribs (geometry b). Ribs inclined at 45º provide lower Nusselt numbers and lower pressure drop. The lowest pressure drop occurs for model with ribbed bottom wall inclined at 45º (geometry c).

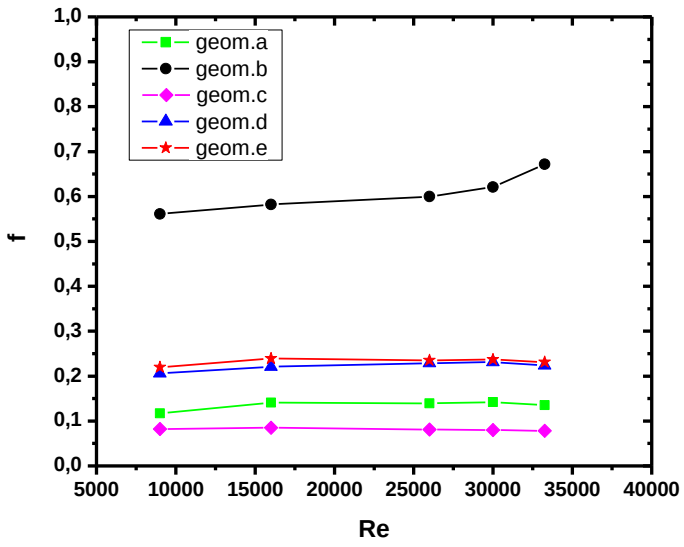

Fig. 12 Equivalent friction coefficient f as a function of Reynolds number for different ribs geometry

CONCLUSION: Advanced experimental techniques, in this case true-color image processing of liquid crystal pattern and particle image velocimetry, allow new approaches to old problems and at the same time open up new areas of research. Image processed data makes available quantitative, full-field information about the distribution of temperature, flow visualization and heat transfer coefficient, which will undoubtedly encourage the study of situation which has been, until now, too complex to consider. The use of the automated isotherm detection method proved to be a reliable tool to simplify LCT measurements and to exclude the arbitrary influence of human interpretation.

Generally, development regions are observed from the entrance up to about three to four inter-rib section in the streamwise direction. Beyond the entrance and exit region, the Nu average numbers exhibit a nearly periodic distribution whose features are strongly related to the rib pitch-to-height ratio and the spanwise coordinate. The corresponding average Nusselt number of the rib-roughened passages is generally two to three times higher in comparison to the smooth channel, so heat transfer performance is better. Correlation of the flow velocity and heat transfer measurements elucidated mechanism limiting heat transfer coefficient for high flow rates. 2-sided ribs set perpendicular to the flow greatly increase turbulence in the flow which enhances the heat transfer but also suffers increase pressure loss.

References

1. Gray G.W. et al. *New cholesteric liquid crystals for information displays*, Electr. Lett., 1973, **9 (26)**, 616
2. Fiebig M. *Vortices: Tools to Influence Heat Transfer – Recent Developments*, Proc. 2nd European Thermal Sciences and 14th UIT National Heat Transfer Conference, 1996, pp 41-56.
3. Fiebig M. *Vortex Generators for Compact Heat Exchangers*, J. of Enhanced Transfer, 1995, Vol. **2**, pp 43-61
4. Moffat R. J. *Experimental Heat Transfer*, Proceedings of The Ninth International Heat Transfer Conference, Jerusalem, Israel 1990, pp 187-205.
5. Han J.C. et al. *An Investigation of Heat Transfer and Friction for Rib-Roughened Surfaces*, Int. J. Heat Mass Transfer, 1978, **21**, pp 1143–1156.
6. Mochizuki S. et al *Effects of Rib Arrangements on Pressure Drop and Heat Transfer in a Rib-Roughened Channel With a Sharp 180 deg Turn*, ASME J. Turbomach., 1997, **119**, pp 610–616.
7. Taslim M.E. et al *45 deg Staggered Rib Heat Transfer Coefficient Measurements in a Square Channel*, ASME J. Turbomach., 1998, **120**, pp 571–580.
8. Chandra P.R. at al *Heat Transfer and Friction Behaviours in Rectangular Channels With Varying Number of Ribbed Walls*, Int. J. Heat Mass Transfer, 2003, **46**, pp 481–495.
9. Park C.W. et al *Heat (Mass) Transfer in a Diagonally Oriented Rotating Two-Pass Channel With Rib-Roughened Walls*, ASME J. Heat Transfer, 2000, **122**, pp 208–211.
10. Cho H.H et al *Local Heat/Mass Transfer Measurements in a Rectangular Duct With Discrete Rbs*, ASME J. Turbomach., 2000, **122**, pp 579–586.
11. Ligrani P.M. et al *Spatially Resolved Heat Transfer and Friction Factors in a Rectangular Channel With 45-deg Angled Crossed-Rib Turbulators*, ASME J. Turbomach., 2003, **125**, pp 575–584.
12. Won S.Y. et al *Spatially Resolved Surface Heat Transfer for Parallel Rib Turbulators With 45 deg Orientations Including Test Surface Conduction Analysis*, ASME J. Heat Transfer, 2004, **126**, pp 193–201.
13. Bailey J. et al *Heat Transfer and Friction in Channels With Very High Blockage 45° Staggered Turbulators*, Proceedings of the ASME Turbo Expo 2003 Power for Land, Sea and Air, Atlanta, GA, 2003, Jun. 16–19
14. Tanda G. et al *Forced Convection Heat Transfer In Channels With Rib Turbulators Inclined at 45 deg*, J. of Turbomachinery, 2009, Vol. **131**, 10 pages
15.Stasiek J. et al *Liquid Crystal Thermography and True-Colour Digital Image Processing*, Optics & Laser Technology, 2006, Vol. **38**, pp 243-256
16. Baughn J.W. et al *Liquid Crystal Methods in Experimental Heat Transfer*, Proceedings of 32nd Heat Transfer and Fluid, California, Mechanics Institute Sacramento, 1991, pp 15-40
17. MINCO Products, Inc., Minnesota, USA
18. MERCK Ltd. Thermochromic Liquid Crystals. Broom Road, Poole, U.K.
19. DATA TRANSLATION Ltd.: Image Processing Handbook, 1991

20. Kowalewski T.A. et al *Temperature Heat Flux*, in: C. Tropea, J. Foss and A. Yarin (Eds.), Handbook of Experimental Fluid Mechanic, Springer-Verlag, Berlin, Heidelberg, 2007, pp 487-561
21. M. Raffel, C. Willert, J. Kompenhans, Particle Image Velocimetry, A Practical Guide, Springer-Verlag, Berlin, 1998
22.Massey B. *Mechanics of Fluids*, Revised by J.Ward-Smith, Stanley Thornes (Publishers) Ltd., United Kingdom, 1989